

# $\Delta^9$ -*cis*-Tetrahydrocannabinol: Natural Occurrence, Chirality, and Pharmacology

Michael A. Schafroth,<sup>†</sup> Giulia Mazzocanti,<sup>†</sup> Ines Reynoso-Moreno,<sup>†</sup> Reto Erni, Federica Pollastro, Diego Caprioglio, Bruno Botta, Gianna Allegrone, Giulio Grassi, Andrea Chicca, Francesco Gasparini, Jürg Gertsch,\* Erick M. Carreira,\* and Giovanni Appendino\*

Cite This: <https://doi.org/10.1021/acs.jnatprod.1c00513>

Read Online

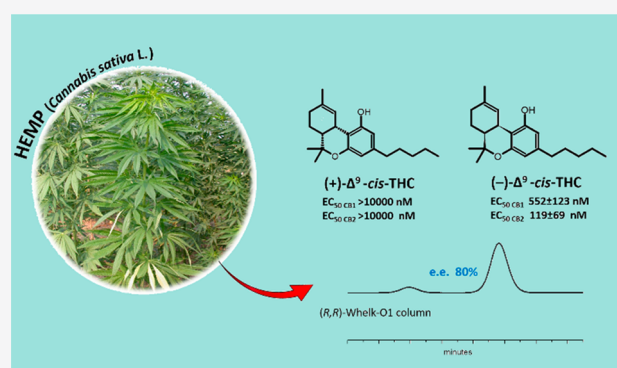
ACCESS |

Metrics & More

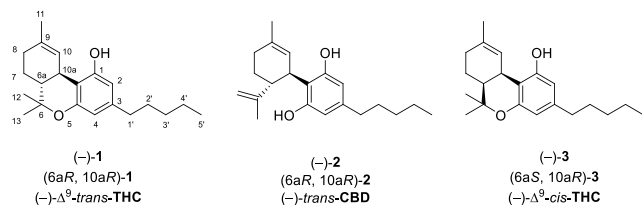
Article Recommendations

Supporting Information

**ABSTRACT:** The *cis*-stereoisomers of  $\Delta^9$ -THC [(−)-3 and (+)-3] were identified and quantified in a series of low-THC-containing varieties of *Cannabis sativa* registered in Europe as fiber hemp and in research accessions of cannabis. While  $\Delta^9$ -*cis*-THC (3) occurs in cannabis fiber hemp in the concentration range of (−)- $\Delta^9$ -*trans*-THC [(−)-1], it was undetectable in a sample of high-THC-containing medicinal cannabis. Natural  $\Delta^9$ -*cis*-THC (3) is scalemic (ca. 80–90% enantiomeric purity), and the absolute configuration of the major enantiomer was established as 6*a*S,10*a*R [(−)-3] by chiral chromatographic comparison with a sample available by asymmetric synthesis. The major enantiomer, (−)- $\Delta^9$ -*cis*-THC [(−)-3], was characterized as a partial cannabinoid agonist in vitro and elicited a full tetrad response in mice at 50 mg/kg doses. The current legal discrimination between narcotic and non-narcotic cannabis varieties centers on the contents of “ $\Delta^9$ -THC and isomers” and needs therefore revision, or at least a more specific wording, to account for the presence of  $\Delta^9$ -*cis*-THCs [(+)-3 and (−)-3] in cannabis fiber hemp varieties.



(−)- $\Delta^9$ -*trans*-Tetrahydrocannabinol [(−)- $\Delta^9$ -*trans*-THC, (−)-1] was first obtained independently in the early 1940s by Adams<sup>1</sup> and by Todd<sup>2</sup> as the major product of the acidic degradation of cannabidiol [CBD, (−)-2]<sup>3</sup> and was identified as the narcotic principle of *Cannabis sativa* L. (Cannabaceae) by Mechoulam two decades later.<sup>4</sup> Based on a correlation with natural (−)-menthol, the configuration of this archetypal “anticipated” natural product was assigned as *trans*, both in its semisynthetic (Šantavý)<sup>5</sup> and in its natural version (Mechoulam).<sup>4</sup>



$\Delta^9$ -Tetrahydrocannabinol has two stereogenic centers (C-6*a* and C-10*a*) and can exist as pairs of enantiomers and diastereomers (two enantiomers of  $\Delta^9$ -*trans*-THC and two enantiomers of  $\Delta^9$ -*cis*-THC, Figure 1). At the outset of modern studies on cannabis, a debate developed regarding the natural occurrence of  $\Delta^9$ -*cis*-THC (3), the identification of the epimerized stereogenic center, and its possible biogenetic

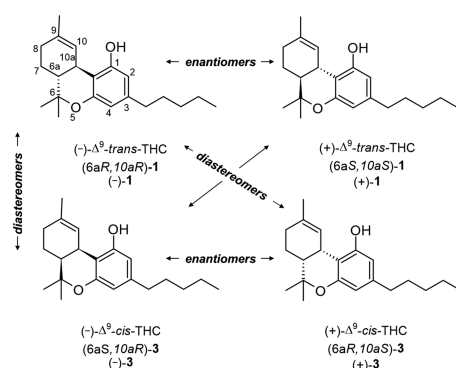


**Figure 1.** Configurational diversity of  $\Delta^9$ -THC derivatives.

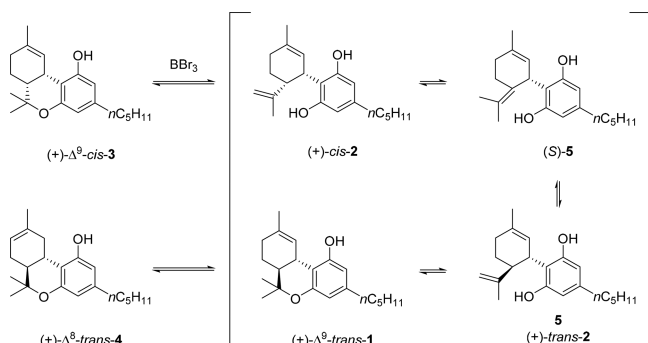
origin. Early reports on the occurrence of  $\Delta^9$ -*cis*-THC (3) in *C. sativa* suffered from the gap between the analytical techniques of the times and the complexity of the cannabinoid bouquet of

Received: May 28, 2021

the plant and could not produce conclusive proof on its occurrence, which was eventually dismissed.<sup>6</sup> Racemic  $\Delta^9$ -*cis*-THC and enantioenriched (+)- $\Delta^9$ -*cis*-THC [(+)-3] were only available by laborious and nonselective syntheses,<sup>6,7</sup> and a relationship with CBD was suggested by the study of its chemistry.

In isomerization experiments with Lewis acids, scalemic (+)- $\Delta^9$ -*cis*-THC [(+)-3] was converted into (+)- $\Delta^8$ -*trans*-THC [(+)-4] of similar enantiopurity (Scheme 1).<sup>8,9</sup> To

**Scheme 1. Isomerization of (+)- $\Delta^9$ -*cis*-THC to (+)- $\Delta^8$ -*trans*-THC According to Razdan and Co-workers**



account for epimerization at C-6a, the authors proposed a reversible isomerization pathway that involved both the cannabidiol olefin isomer 5 and cannabidiol 2 as intermediates (Scheme 1).<sup>8,9</sup> This result suggested that  $\Delta^9$ -*cis*-THC could originate from CBD or at least that it could be biogenetically related to this compound. In the late 1970s, a paper by Smith and Kempfert described the isolation of  $\Delta^9$ -*cis*-THC from various seized samples of what they referred to as marijuana, observing a direct correlation between the concentrations of  $\Delta^9$ -*cis*-THC and CBD [(-)-2].<sup>10</sup> On account of previous work on the isomerization of (+)- $\Delta^9$ -*cis*-THC to (+)- $\Delta^8$ -*trans*-THC via an olefin isomer of CBD (5) (Scheme 1), an artifactual origin could not be dismissed. This, along with uncertainties on the absolute configuration of the natural product, made this work largely overlooked by the broader scientific community, to the point that in 2018 the Expert Committee on Drug Dependence (ECDD) of the WHO concluded that “the stereoisomer (–)-*trans*- $\Delta^9$ -THC (*sic*) is the only one that occurs naturally in the cannabis plant and is generally the only stereoisomer that has been studied”.<sup>11</sup> If the presence of  $\Delta^9$ -*cis*-THC in cannabis were to be confirmed, this compound would fall under the umbrella definition of “THC isomers” currently used to sort out non-narcotic cannabis fiber hemp strains from narcotic cannabis,<sup>12</sup> highlighting the forensic relevance of a definitive resolution of the *cis*-THC issue.

**Table 1. GC Quantitation (% w/w) of CBD,  $\Delta^9$ -*cis*-THC,  $\Delta^9$ -*trans*-THC, and CBN in Various Cannabis Fiber Hemp Strains and Research Accessions of Cannabis**

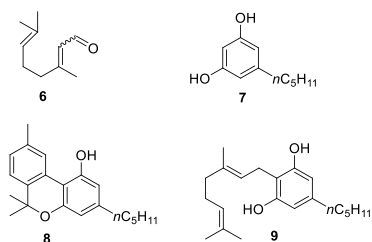
hemp strain	CBD (2)	$\Delta^9$ - <i>cis</i> -THC (3)	$\Delta^9$ - <i>trans</i> -THC (1)	<i>trans/cis</i> ratio	CBN (7)	CBG (8)
Beniko	0.773	0.0190	0.0348	1.8	0.0719	
Bialobrzieskie	0.766	0.0195	0.0364	1.9	0.0103	
Carma	2.43	0.0802	0.104	1.3	0.125	
Carmagnola	3.67	0.0967	0.158	1.6	0.0675	
Carmaleonte	4.17	0.0115	0.0161	1.4	0.0183	1.90
Chamaeleon	1.16	0.0311	0.0581	1.9	0.0208	
CRA_1 Eletta Campana	2.62	0.0648	0.124	1.9	0.0214	0.272
CRA_5 Fibranova	4.90	0.141	0.199	1.4	0.0771	0.398
Delta-Ilosa	1.26	0.0349	0.0553	1.6	0.0114	2.17
Denise	7.10	0.0153	0.120	7.8	0.0238	
Epsilon 68	1.123	0.0328	0.0607	1.9	0.0224	
Fedora 17	1.89	0.0380	0.0699	1.8	0.0183	
Felina 32	1.43	0.0366	0.0629	1.7	0.0248	
Férimon	1.32	0.0280	0.0542	1.9	0.0116	
Fibrinol	0.884	0.0212	0.0339	1.6	0.0151	
Finola	1.84	0.0449	0.229	5.1	0.0937	
Futura 75	1.40	0.0393	0.0797	2.0	0.0219	
Ivory	9.06	0.0176	0.0397	2.3	0.0109	
KC Dora	2.16	0.0650	0.908	14.0	0.164	
Kompolti	3.95	0.122	0.182	1.5	0.0602	
Lovrin 110	1.36	0.0343	0.0651	1.9	0.0146	0.109
Marcello	2.02	0.0419	0.241	5.8	0.0483	
Markant	9.57	0.0216	0.0415	1.9	0.0170	
Monoica	1.41	0.0321	0.0571	1.8	0.0182	0.0780
Santhica 27	0.0120	0.000268	0.000400	1.5		1.35
Tiborszallasi	2.75	0.0673	0.123	1.8	0.0278	0.168
Tigra	0.841	0.0213	0.0890	4.2	0.0219	
Tisza	2.32	0.0501	0.4360	8.7	0.277	
Uniko B	1.27	0.0254	1.55	61.0	0.359	
Uso 31	0.592	0.0115	0.0224	1.9	0.0679	0.0980
Zenit	2.75	0.00880	0.0149	1.7	0.00510	

Limited information also exists on the pharmacology of  $\Delta^9$ -*cis*-THCs and their potential use in medicine. In 1971, Mechoulam reported that racemic synthetic  $\Delta^9$ -*cis*-THC was inactive in behavioral tests in rhesus monkeys,<sup>13</sup> and a few years later Razdan and Martin showed that (+)- $\Delta^9$ -*cis*-THC was mostly inactive in tests for overt behavior in dogs, with potencies being reduced 100-fold compared to (-)- $\Delta^9$ -*trans*-THC.<sup>14</sup> Similarly, racemic  $\Delta^9$ -*cis*-THC was reported to be 20-fold less potent than natural (-)- $\Delta^9$ -*trans*-THC in the “popcorn assay”, a rarely used mouse model of cannabinoid activity based on the association of ataxia and hyperexcitability to touch.<sup>15</sup>

To address these unanswered questions, we have quantified  $\Delta^9$ -*cis*-THCs in various hemp samples, assessing its absolute configuration and enantiomeric purity by chiral chromatographic comparison with an enantiopure (-)- $\Delta^9$ -*cis*-THC sample available by asymmetric synthesis. By capitalizing on an enantio- and diastereoselective synthesis of all  $\Delta^9$ -THC stereoisomers (Figure 1),<sup>16</sup> we next comparatively investigated the bioactivity profile of both  $\Delta^9$ -*cis*-THC enantiomers toward cannabinoid receptors (CB1, CB2) and endocannabinoid degrading enzymes (FAAH, MAGL, ABHD6, and ABDH12) in vitro. The major enantiomer, (-)- $\Delta^9$ -*cis*-THC, was further evaluated in vivo for its cannabinomimetic effect in the “tetrad test”.

## RESULTS AND DISCUSSION

We were unable to obtain a sufficiently pure sample of natural  $\Delta^9$ -*cis*-THC by isolation from the hemp strain Carmagnola, even though it turned out to be relatively rich in this compound (see below). An authentic standard of racemic  $\Delta^9$ -*cis*-THC was obtained by the reaction of citral (6) and olivetol (7) under acidic conditions (see Scheme S1, Supporting Information for a mechanistic rationalization of the reaction).<sup>7,8</sup> An analytically pure, totally synthetic sample was used to develop a GC-MS/MS method to quantify ( $\pm$ )- $\Delta^9$ -*cis*-THC in the presence of ( $\pm$ )- $\Delta^9$ -*trans*-THCs and other phytocannabinoids.  $\Delta^9$ -*cis*-THC (3) was then quantified in the flower heads of a selection of cannabis samples encompassing both registered fiber hemp varieties and research accessions, two of which (UniKoB and KC Dora) would be classified as narcotics because of their relatively high concentration of  $\Delta^9$ -*trans*-THC (Table 1). Along with  $\Delta^9$ -*cis*-THC (3),  $\Delta^9$ -*trans*-THC (1), cannabidiol (CBD, 2), cannabinol (CBN, 8), and cannabigerol (CBG, 9) were quantified.



Cannabidiol (2) was the major phytocannabinoid in all samples, where, remarkably,  $\Delta^9$ -*cis*-THC (3) could also be detected in amounts comparable (around 1:2) to that of  $\Delta^9$ -*trans*-THC (Table 1). A direct relationship seems to exist between the concentration of *trans*- $\Delta^9$ -THC and the *trans/cis*-THC ratio, since in the two narcotic samples analyzed, enrichment in the *trans*-isomer was associated with an increase

of the *trans/cis* ratios, from an average value of ca. 2:1 to ca. 61:1 (UniKoB) and 14:1 (KC Dora).

These results were confirmed by the detection of ( $\pm$ )- $\Delta^9$ -*cis*-THC (3) by reversed-phase ultra-high-performance liquid chromatography (RP-UHPLC) in two additional strains (Fibranova, Orange) and in two strains already analyzed by GC-MS/MS (Futura 75, Kompolti) (Table 2, Figure 2).

**Table 2.** ( $\pm$ )- $\Delta^9$ -*cis*-THC (3) Content in Cannabis Strains Characterized by Different Concentrations of CBD (2) and ( $\pm$ )- $\Delta^9$ -*trans*-THC (1), with Obtained Data by RP-UHPLC Analysis

	CBD % (w/w)	( $\pm$ )- $\Delta^9$ - <i>cis</i> -THC (3) % (w/w)	( $\pm$ )- $\Delta^9$ - <i>trans</i> -THC (1) % (w/w)	<i>trans/cis</i> ratio
Bedrocan	0.16		22.0	
Orange	13.5	0.12	0.33	2.8
Fibranova	3.95	0.11	0.18	1.6
Kompolti	3.85	0.09	0.17	1.9
Futura 75	1.42	0.04	0.09	2.3

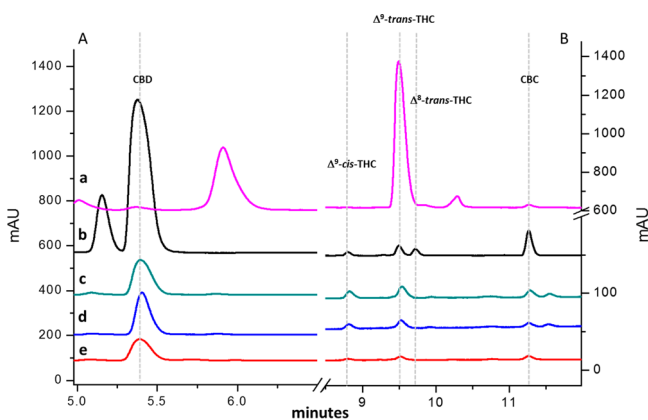


**Figure 2.** Crude plant ethanol extracts of cannabis strains [(a) Bedrocan; (b) Orange; (c) Fibranova; (d) Kompolti; (e) Futura 75], analyzed on a Titan (100 mm  $\times$  2.1 mm, 1.9  $\mu$ m) column. (A) Retention time zone of CBD (from minute 5 to 7.5). (B) Retention time zone of THC (from minute 8.5 to 12).

Remarkably, the concentration of ( $\pm$ )- $\Delta^9$ -*cis*-THC was below the limits of detection in Bedrocan, a high (-)- $\Delta^9$ -*trans*-THC [(-)-1] medicinal cannabis strain. It is possible that the contrasting data on the occurrence of ( $\pm$ )- $\Delta^9$ -*cis*-THC in cannabis are related to its presence in non-narcotic low-THC-containing fiber hemp varieties rather than in narcotic high-THC-containing cannabis strains, for which their investigation has long dominated the analytics of cannabis. To determine that no additional compound coeluted with ( $\pm$ )- $\Delta^9$ -*cis*-THC under the UHPLC analysis, two distinct and complementary strategies were pursued. The first was based on “ultra-resolution” chromatography using four columns in series to gain resolution by increasing the time of analysis (Figure S5, Supporting Information). The second one involved the use of a chromatographic system (see Experimental Section) coupled to a high-resolution mass spectrometer (HRMS) and was based on comparison of retention time and accurate mass measurements with a reference standard, a precaution dictated by the isobaric state of many phytocannabinoids (Figure S6, Supporting Information). Taken together, the results from GC and RP-UHPLC coupled with HRMS showed unambiguously

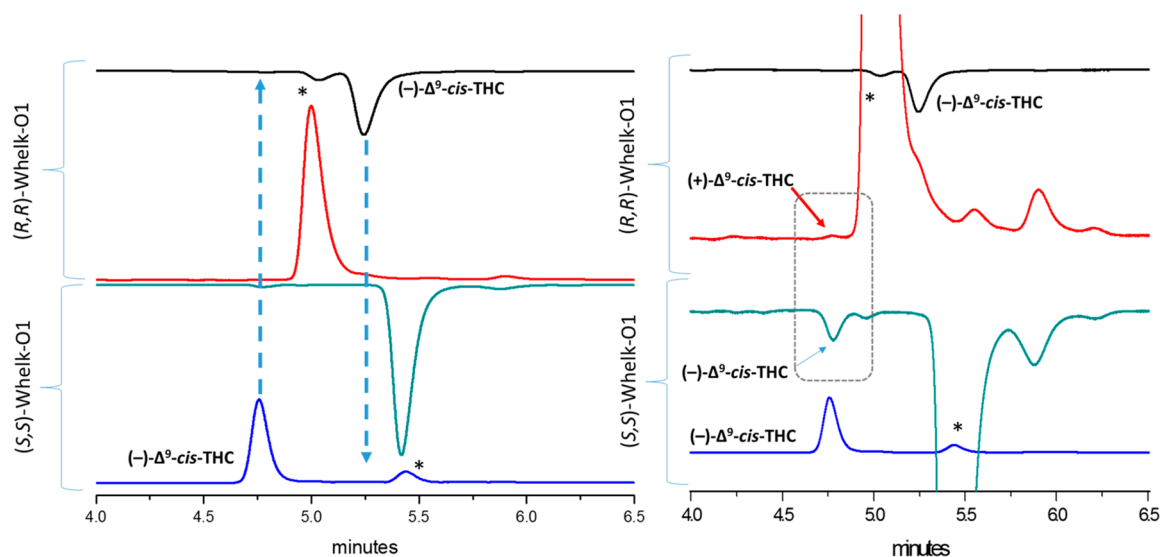


**Figure 3.** A crude plant ethanol extract (namely, Futura 75) was analyzed by applying the ICCA protocol. The chromatogram of  $(-)\text{-}\Delta^9\text{-cis-THC}$  [( $-$ )-3] spiked with CBD (2) (marked with an asterisk) has been added for peak identification. The dashed lines indicate the retention time of the  $(+)\text{-}\Delta^9\text{-cis-THC}$  (if present) on the column with inverted chirality. In the inset (on the right) it is possible to identify and integrate (on the  $(R,R)$ -Whelk-O1 column) the peak relative to  $(+)\text{-}\Delta^9\text{-cis-THC}$  [( $+$ )-3] (pointed with a red arrow).

that  $(\pm)\text{-}\Delta^9\text{-cis-THCs}$  (3) and  $(\pm)\text{-}\Delta^9\text{-trans-THCs}$  (1) co-occur in cannabis fiber hemp strains.

To establish the absolute configuration and the enantiomeric excess of naturally occurring  $\Delta^9\text{-cis-THC}$ , which could also provide insights into its biogenetic origin (vide infra), we developed an enantioselective analytical method that was able to separate the different  $\Delta^9\text{-cis-THC}$  enantiomers. To this end, the inverted chirality column approach (ICCA) in normal-phase enantioselective ultra-high-performance liquid chromatography (NP-eUHPLC) was used.<sup>17,18</sup> This method is based on the analysis of a chiral compound on two columns having enantiomeric chiral stationary phases, which are, therefore, identical in terms of thermodynamics (retention factor and selectivity) and kinetics (efficiency) but show opposite affinity for enantiomeric compounds, in accordance with the reciprocal principle of selectand–selector systems.<sup>19</sup> Thus, a column switch will result in inverted retention times for a pair of enantiomers, making it possible to identify enantiomers and evaluate enantiomeric excesses even when only one enantiomer of a chiral compound is available. To implement this strategy, samples of synthetic  $(-)\text{-}\Delta^9\text{-cis-THC}$  [( $-$ )-3]<sup>16</sup> as well as  $(-)\text{-CBD}$  [( $-$ )-2] were analyzed in the popular hemp strain Futura 75 on two columns  $(R,R)$ -Whelk-O1 and  $(S,S)$ -Whelk-O1, which met the ICCA requirements (Figure 3).

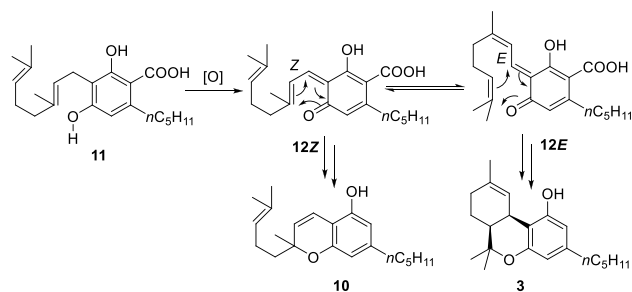
On the  $(S,S)$ -Whelk-O1 column,  $(-)\text{-}\Delta^9\text{-cis-THC}$  [( $-$ )-3] eluted at 4.75 min, which is well before CBD (2), the main phytocannabinoid constituent of the extract (Figure 3, blue trace = standards; green trace = extract). In accordance with the ICCA protocol,<sup>18</sup>  $(+)\text{-}\Delta^9\text{-cis-THC}$  [( $+$ )-3] (red trace) eluted at the same retention time on the  $(R,R)$ -Whelk-O1 column. On comparison of the area integration of the  $(-)$ -enantiomer [( $-$ )-3] on the  $(S,S)$ -Whelk-O1 column and that of the  $(+)$ -enantiomer [( $+$ )-3] on the  $(R,R)$ -Whelk-O1 column, an enantiomeric excess of 79.8% was established, with the  $(-)$ -enantiomer being more abundant. The presence of  $\Delta^9\text{-cis-THC}$  (3) as a scalemic mixture was also confirmed by enantioselective supercritical fluid chromatography (eSFC) analysis. It has already been shown that eSFC shows superior chemo- and diastereoselectivity in the analysis of phytocanna-

binoids,<sup>18</sup> as additionally demonstrated by the separation of  $(-)\text{-CBD}$  from the  $\Delta^9\text{-cis-THC}$  enantiomers using a column with the Whelk-O1 selector in eSFC conditions reported in the **Experimental Section**. Thus, an eSFC method allowed resolution of both enantiomers of  $\Delta^9\text{-cis-THC}$  (3, Figure S9a, **Supporting Information**), without interference from  $(-)\text{-CBD}$ . The peaks were assigned to the respective enantiomers by co-injection with authentic standards (Figure S9b and c, **Supporting Information**). Two fiber hemp strains (Kompolti and CRA\_05 Fibranova) were then analyzed (Figure S9d–g in **Supporting Information**), measuring an enantiomeric excess for natural  $\Delta^9\text{-cis-THC}$  of 88.8% (Kompolti) and 85.6% (CRA\_05 Fibranova), confirming the  $(-)$ -enantiomer as more abundant.

Taken together, the results from analytical chromatography show that  $\Delta^9\text{-cis-THC}$  (3) occurs in cannabis fiber hemp strains as a scalemic mixture, providing a clue of its biogenetic origin. Examples of scalemic<sup>20</sup> or racemic<sup>21</sup> natural products have been reported previously. This raises the question of the existence of a specific oxido-cyclase similar to those responsible for the formation of cannabidiol [CBD, ( $-$ )-2] and  $(-)\text{-}\Delta^9\text{-trans-THC}$  [( $-$ )-1].<sup>22</sup> Alternatively, a biogenetic relationship between  $\Delta^9\text{-cis-THC}$  (3) and cannabichromene (CBC, 10) may exist. Cannabichromene (CBC) is the only phytocannabinoid that has been converted under laboratory conditions (excess of  $\text{BF}_3$  in DCM) into  $\Delta^9\text{-cis-THC}$ , along with a host of other rearrangement products.<sup>15,23</sup> CBC is highly scalemic or even racemic and is not present in significant amounts in cannabis flower heads, being produced mostly in the early stages of development of the plant.<sup>23</sup> Given also the very low yield and harsh conditions required for the chemical conversion, derivation of  $\Delta^9\text{-cis-THC}$  from CBC seems unlikely. However, it is possible that  $\Delta^9\text{-cis-THC}$  (3) and CBC (10) are derived from alternative pericyclic processes from cannabigerolic acid (11). Upon FAD-promoted hydride abstraction, intramolecular hetero-Diels–Alder cycloaddition of the quinone methide 12-*E* would afford, after decarboxylation,  $\Delta^9\text{-cis-THC}$  (3), while electrocyclization of 12-*Z* would generate, after decarboxylation, cannabichromene

(CBC, 10) (Scheme 2). Since the electrocyclicization of CBC (10) is thermally reversible,<sup>21</sup> the possibility exists that during

**Scheme 2. Alternative Pericyclic Conversion of the CBG-Derived Quinone Methide 12 to  $\Delta^9$ -*cis*-THC (3) and CBC (10)**



decarboxylation of the native acidic form of CBC a substantial erosion of optical purity takes place, explaining the higher scalemic state of CBC compared to  $\Delta^9$ -*cis*-THC.

To evaluate the bioactivity of the different THC stereoisomers, binding affinities and functional activities at both cannabinoid receptors, as well as the effectiveness in inhibiting enzymes involved in the degradative endocannabinoid metabolism (FAAH, MAGL, ABHD6, ABHD12), were evaluated for both enantiomers of  $\Delta^9$ -*cis*-THC, and the results were compared to those of (–)- $\Delta^9$ -*trans*-THC. At the cannabinoid receptors CB1 and CB2, (–)- $\Delta^9$ -*cis*-THC showed 10-fold lower binding affinities in both the binding assay and the functional assay.<sup>24</sup> In contrast, (+)- $\Delta^9$ -*cis*-THC was inactive in both assays, showing binding affinities as well as functional activities only in the high micromolar range. Among the other components of the endocannabinoid system, (–)- $\Delta^9$ -*cis*-THC showed similar weak inhibition of the anandamide and 2-AG hydrolytic enzymes (FAAH, ABHD6, and ABHD12) to (–)- $\Delta^9$ -*trans*-THC. Interestingly, the (+)-*cis*-isomer only showed inhibition for ABHD6 and ABHD12. In general, the  $IC_{50}$  value for these natural tetrahydrocannabinols at the endocannabinoid degradative enzymes was higher than the concentrations reached in vivo after cannabis consumption.<sup>25</sup> Nevertheless, the inhibition of ABHD12 is noteworthy and might serve as an entry point for the development of reversible inhibitors through rigorous medicinal chemistry efforts. Overall, the concomitant inhibition of FAAH and ABHD6 and -12 may suggest a privileged interaction with multiple targets in the endocannabinoid system, as shown previously for other chemical scaffolds.<sup>26</sup>

The potential cannabimimetic effects of the major isomer [(–)- $\Delta^9$ -*cis*-THC, (–)-3] was further assessed in vivo and compared to the effects of (–)- $\Delta^9$ -*trans*-THC [(–)-1] in a battery of four tests typically associated with CB1 receptor activation in mice (hypothermia, catalepsy, hypolocomotion, and analgesia), the so-called “tetrad test”. Experiments using equipotency to (–)- $\Delta^9$ -*trans*-THC as the end-point showed that (–)- $\Delta^9$ -*cis*-THC could elicit the full tetrad in BALB/c mice upon intraperitoneal injection at 50 mg/kg (Figure 4). For comparison,  $\Delta^9$ -*trans*-THC showed similar potencies at a 6–10 mg/kg dose, in agreement with the different potencies measured in vitro for CB1 receptor activation.

**Table 3. In Vitro Comparative Biological Evaluation of (–)- $\Delta^9$ -*trans*-THC (1) and the Enantiomers of  $\Delta^9$ -*cis*-THC for CB1/CB2 Binding ( $K_i$ ) and Functional Activity ( $EC_{50}$  [<sup>35</sup>S]GTP $\gamma$ S Binding) and for Inhibition of the Endocannabinoid Degrading Enzymes ( $IC_{50}$  Values)**

CB1 and CB2 receptor binding affinities in radiolabel assay with [ <sup>3</sup> H] CP55940 ( $K_i$ , nM)			
	(–)- $\Delta^9$ - <i>trans</i> -THC	(–)- $\Delta^9$ - <i>cis</i> -THC	(+)- $\Delta^9$ - <i>cis</i> -THC
CB1	22 ± 13	228 ± 45	2900 ± 421
CB2	47 ± 11	99 ± 29	4750 ± 261
CB1 and CB2 receptor functional activities in [ <sup>35</sup> S]GTP $\gamma$ S binding assay ( $EC_{50}$ , nM)			
	(–)- $\Delta^9$ - <i>trans</i> -THC	(–)- $\Delta^9$ - <i>cis</i> -THC	(+)- $\Delta^9$ - <i>cis</i> -THC
CB1	43 ± 30 (partial) <sup>a</sup>	552 ± 123 (partial) <sup>a</sup>	>10 000
CB2	12 ± 7 (partial) <sup>a</sup>	119 ± 69 (partial) <sup>a</sup>	>10 000
inhibition of endocannabinoid degrading enzymes ( $IC_{50}$ , $\mu$ M)			
	(–)- $\Delta^9$ - <i>trans</i> -THC	(–)- $\Delta^9$ - <i>cis</i> -THC	(+)- $\Delta^9$ - <i>cis</i> -THC
FAAH	43.6 ± 3.5	36.3 ± 2.7	>80
MAGL	>100	>100	>100
ABHD6	48.2 ± 3.0	39.8 ± 4.8	35.1 ± 4.1
ABHD12	11.6 ± 1.8	14.1 ± 2.6	28.8 ± 5.7

<sup>a</sup>Partial = partial agonist compared to the full agonist CP55940.

## CONCLUSIONS

The power of enantio- and diastereodivergent synthesis for the first time provided convenient access to all four stereoisomers of  $\Delta^9$ -THC and has enabled phytochemical and pharmacological investigations. We have established that all four stereoisomers of  $\Delta^9$ -THC (Figure 1) are natural products with the selective accumulation of the (–)-*trans* isomer in narcotic cannabis and comparable occurrence of the (–)-*trans* and the (–)-*cis*-isomers in cannabis fiber hemp strains. In a sample of medicinal cannabis (Bedrocan),  $\Delta^9$ -THC is produced in very high enantiomeric purity (ee >99%) and exclusively in the *trans*-form.<sup>18</sup> Conversely, in 34 samples of cannabis varieties where CBD (2) or CBG (8) was the predominant phytocannabinoid,  $\Delta^9$ -THC was produced in lower diastereomeric purity as a mixture<sup>17</sup> of *trans*- and scalemic *cis*-isomers. On the basis of its scalemic nature, we hypothesize that  $\Delta^9$ -*cis*-THCs (3) are produced either by a nonselective oxidocyclase activity like that involved in the biosynthesis of CBD (2) and  $\Delta^9$ -*trans*-THC (1) or alternatively by a pericyclic cyclase activity like the one involved in the formation of CBC, a highly scalemic or even racemic phytocannabinoid.

$\Delta^9$ -*cis*-THC (3) is a weak but, nevertheless, efficacious cannabimimetic agent as established in the tetrad test in vivo. Low-dose  $\Delta^9$ -*trans*-THC has been shown to elicit beneficial therapeutic effects with reduced side effects;<sup>27</sup> thus, the less potent (–)- $\Delta^9$ -*cis*-THC could retain some of the desired therapeutic effects of  $\Delta^9$ -*trans*-THC. The legal status of  $\Delta^9$ -*cis*-THC is, however, unclear. The current legal discrimination between narcotic and non-narcotic cannabis varieties centers on the content of “ $\Delta^9$ -THC and isomers” and is based on the chromatographic (GC or HPLC) determination of  $\Delta^9$ - and  $\Delta^8$ -*trans*-tetrahydrocannabinols.<sup>28,29</sup>  $\Delta^9$ -*cis*-THCs (3) are not expected to interfere with these assays, since their chromatographic behavior is distinct from that of the *trans*-THCs.<sup>30</sup> On the other hand, 3 could interfere with radioimmune assays for narcotic cannabinoids,<sup>28</sup> as well as in the forensic *p*-aminophenol assay (4-AP test) for narcotic

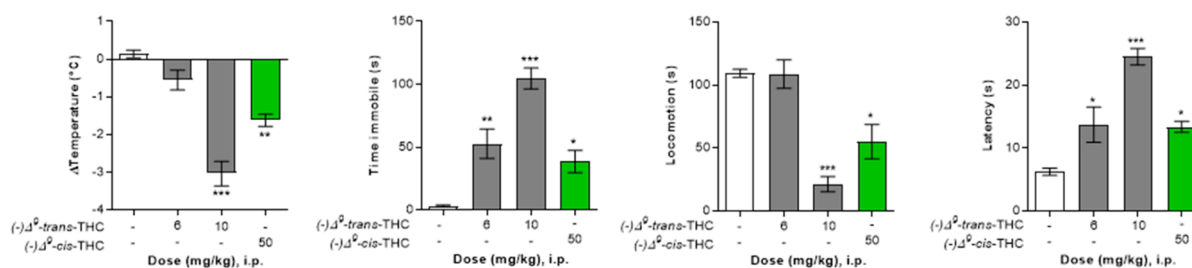


**Figure 4.** CB1 receptor dependence of the pharmacological effects of  $(-)\Delta^9$ -*cis*-THC and  $(-)\Delta^9$ -*trans*-THC in mice. (A) Hypothermia; (B) catalepsy-like behavior; (C) hypolocomotion; and (D) analgesia elicited by  $(-)\Delta^9$ -*trans*-THC (gray) and  $(-)\Delta^9$ -*cis*-THC (green) compared with vehicle control (white) in BALB/c male mice 1 h after intraperitoneal injection. The data of  $(-)\Delta^9$ -*trans*-THC are reported for comparison (published in ref 21). Doses are expressed in mg/kg. Data show means  $\pm$  SD. Groups were compared to the vehicle-treated control group using the Kruskal–Wallis test, followed by the Mann–Whitney test,  $n = 6$ –15 mice per group. \*\*\* $p < 0.001$ , \*\* $p < 0.01$ , \* $p < 0.05$  versus vehicle.

cannabis.<sup>30</sup> Furthermore, since the metabolism of *cis*-THCs is unknown, the metabolites could interfere with the current forensic tests for cannabis intoxication based on the detection of its 11-*nor*-9-carboxy derivative.<sup>28</sup> Furthermore, since  $\Delta^9$ -*cis*-THCs (**3**) are “isomers” of  $\Delta^9$ -*trans*-THC (Figure 1), they should, in principle, be accounted for in the forensic evaluation of cannabis strains.<sup>31</sup> A revision, or at least a more specific definition, of the markers used for the legal classification of cannabis strains will therefore be needed to account for the presence of significant amounts of  $\Delta^9$ -*cis*-THC in cannabis fiber hemp varieties, adapting accordingly the stereochemical polysemy of the term “ $\Delta^9$ -THC”.

## EXPERIMENTAL SECTION

**General Experimental Procedures.** Silica gel 60 (70–230 mesh) and Merck 60 F254 (0.25 mm) TLC plates used for the phytochemical and the synthetic activities were purchased from Merck (Germany). Ethyl acetate, petroleum ether, ethanol, ethyl ether, and all reagents were purchased from Sigma-Aldrich (Italy).

**Plant Material.** All samples were supplied by Canvasalus Research (Monselice (PD), Italy) and were identified by Dr. Gianpaolo Grassi. Voucher specimens of all samples analyzed are stored at Canvasalus Research.

**$\Delta^9$ -*cis*-THC.** The racemic compound was prepared according to ref 6. An analytical sample was obtained by semipreparative HPLC by using an (S,S)-Whelk-O2 column (10  $\mu$ m, 250 mm  $\times$  10 mm L  $\times$  i.d.) (Regis Technologies, Morton Grove, IL, USA), using a mixture of *n*-hexane/isopropanol (99.5:0.5% v/v) as eluent (flow rate 4.0 mL/min and  $T_{col}$  25  $^{\circ}$ C). The purification took place in a single step and provided a product with a purity of  $\geq 95\%$ . The pure enantiomers were available from previous synthetic work.<sup>16</sup>

**Extraction.** The dried plant material (500 mg) was decarboxylated by heating to 130  $^{\circ}$ C for 2 h in a glass test tube. The plant material was then extracted with analytical grade ethanol (20 mL) in an ultrasound bath for 30 min. The extract was filtered through a 0.45  $\mu$ m PTFE membrane and then analyzed.

**GC-MS Analysis.** GC-MS analysis was carried out on a Trace GC apparatus coupled to a Polaris Q ion trap mass spectrometer (Thermo Finnigan, San José, CA, USA). The gas chromatograph was operated in split mode using a 1  $\mu$ L injection with the injector set and maintained at 270  $^{\circ}$ C. Helium was used as carrier gas at a flow rate of 1.0 mL/min. The separation was performed on a TG-5MS capillary column (30 m, 0.25 mm i.d., 0.25 mm thickness) (Thermo Fisher Scientific). The oven column temperature was programmed as follows: the initial temperature of 150  $^{\circ}$ C was maintained for 2 min and was next increased from 150  $^{\circ}$ C to 270  $^{\circ}$ C at a rate of 5  $^{\circ}$ C/min, eventually maintaining it at 270  $^{\circ}$ C for 15 min. Electron ionization (EI) was operated at 70 eV. The transfer line and ion source were kept at 270 and 250  $^{\circ}$ C, respectively. The MS was used in full scan ( $m/z$  33–650) and in tandem MS/MS mode. Standard solutions of CBD, CBN, and CBG were added to tribenzylamine (100  $\mu$ g/mL) as

internal standards and then analyzed in full scan modality, and calibration curves were linear in the range 20–2000  $\mu$ g/mL for CBD and CBG and 5–200  $\mu$ g/mL for CBN.  $\Delta^9$ -*cis*-THC and  $\Delta^9$ -*trans*-THC standard solutions, added to tribenzylamine (100  $\mu$ g/mL), were analyzed in MS/MS modality with the following same selected parent/daughter ions transitions:  $m/z$  314  $\rightarrow$  299 and  $m/z$  314  $\rightarrow$  243. Calibration curves obtained were linear in the range 1–200  $\mu$ g/mL.

**Achiral RP-UHPLC-HRMS Analysis.** Standard solutions in methanol of  $(-)$ -*trans*-cannabidiol, cannabinol,  $(-)$ -*trans*- $\Delta^9$ -THC, and ( $\pm$ )-cannabichromene were purchased from Cerilliant (Round Rock, TX, USA) as methanol solutions (0.1–1.0 mg/mL) with a  $\geq 99\%$  purity. All solvents used for UHPLC analyses were LC-MS grade and were purchased from Sigma–Aldrich (St. Louis, MO, USA) as well as formic acid (FA). UHPLC analyses were performed on a Shimadzu Nexera UHPLC system (Shimadzu, Milano, Italy). The Shimadzu Nexera UHPLC was composed of a CBM-20A controller, a SIL-30AC autosampler, four LC-30AD dual-plunger parallel-flow pumps, a DGU-20A5 vacuum degasser, and an SPD-M20A photodiode array detector (equipped with a semimicro flow cell of 2.5  $\mu$ L). The system was controlled by LabSolution software (Shimadzu, Milan, Italy). UHPLC-HRMS analysis was achieved using an UltiMate 3000RSLC nano LC (Dionex, Benelux, Amsterdam, The Netherlands) furnished with a binary rapid separation capillary flow pump and a ternary separation loading pump (NCP-3200RS UltiMate3000). Only the loading pump was employed in this study. Mass detection was performed using an Exactive Orbitrap (Thermo Fisher Scientific, Waltham, MA, USA) at a mass range of  $m/z$  200–2000.

Mass acquisition was set as follows: resolution of 100,000 at  $m/z$  200, positive ESI mode, sheath gas flow of 5 units, spray voltage 3.5 kV, capillary voltage 77.5 V, capillary temperature 300  $^{\circ}$ C, and tube lens voltage at 250 V. Software tools were from Thermo Fisher Scientific (Waltham, MA, USA). Specifically, instrument operation, chromatographic data acquisition, and processing were performed using the Chromeleon 6.8 chromatography data system, while mass spectra were processed using Xcalibur. All separations were performed by using Titan C<sub>18</sub> columns packed with 1.9  $\mu$ m fully porous particles of narrow particle size distribution. The mobile phase consisted of water (A) and acetonitrile (B), both containing 0.1% FA. The elution gradient was set as follows: (a) For UHPLC-HRMS analysis 70% B (0 min), 70% B (1 min), 100% B (21 min), 100% B (25 min), 70% B (26 min), and 70% B (36 min). The flow rate was 0.25 mL/min for one Titan C<sub>18</sub> column (100  $\times$  2.1 mm L  $\times$  i.d.). The column oven was set at 30  $^{\circ}$ C. A volume of 1  $\mu$ L was injected. (b) For ultraresolution, the separation gradient was 70% B (0 min), 70% B (1 min), 100% B (61 min), 100% B (65 min), 70% B (66 min), and 70% B (76 min). The flow rate was 0.5 mL/min for four Titan C<sub>18</sub> columns (100  $\times$  3.0 mm L  $\times$  i.d.). The column oven was set at 30  $^{\circ}$ C. A volume of 2  $\mu$ L was injected.

**Enantioselective NP-eUHPLC Chromatographic Analysis and ICCA Application.** All solvents used for UHPLC analyses were HPLC grade and were purchased from Sigma–Aldrich. UHPLC

analyses were performed on an UltiMate 3000RSLC (Dionex, Benelux, Amsterdam, The Netherlands). Specifically, instrument operation and chromatographic data acquisition and processing were performed using the Chromeleon 7.2 chromatography data system. All separations were performed by using (*R,R*)-Whelk-O1 and (*S,S*)-Whelk-O1 CSPs, prepared according to a previously described procedure starting from Kromasil 1.8  $\mu\text{m}$  silica particles and slurry packed into 100  $\times$  4.6 mm (L  $\times$  i.d.) stainless steel columns. Isocratic conditions were set as follows: mobile phase: *n*-hexane/isopropanol (99.5:0.5 v/v); flow rate: 1.0 mL/min; *T* = 30  $^{\circ}\text{C}$ ; detection: UV 214 nm.

**Enantioselective SFC.** Synthetic ( $-$ )- $\Delta^9$ -*cis*-THC and ( $\pm$ )- $\Delta^9$ -*cis*-THC were prepared according to previously published methods, and standard solutions thereof were prepared in acetonitrile (0.4 mg/mL).<sup>16,19</sup> Extracts of two cannabis fiber hemp strains (Kompolti and CRA\_05 Fibranova) were purified by preparative thin-layer chromatography (Merck silica gel 60 F254 TLC glass plates, visualized with 254 nm light and cerium ammonium molybdate solution followed by heating), isolating the ( $\pm$ )- $\Delta^9$ -*cis*-THC-containing fraction ( $R_f$  = 0.23, hexanes/ethyl acetate, 15:1). Solutions of purified extracts were prepared in acetonitrile (1.4–1.6 mg/mL). eSFC analyses were conducted on a Waters Acquity UPC<sup>2</sup> analytical SFC with a diode array detector. Data were analyzed and processed using the Empower 3 software suite. Enantiomeric excess was determined by eSFC; stationary phase: (*R,R*)-Whelk-O1 (5  $\mu\text{m}$ , 250  $\times$  4.6 mm L  $\times$  i.d., Regis Technologies, Norton Grove, IL, USA); mobile phase: CO<sub>2</sub>/isopropanol, 95.0:5.0, v/v; flow rate: 2.0 mL/min; temperature = 40  $^{\circ}\text{C}$ ; detection: UV 220 nm. The peaks were assigned to (+)- $\Delta^9$ -*cis*-THC (12.2 min) and ( $-$ )- $\Delta^9$ -*cis*-THC (13.2 min) by co-injection of ( $-$ )- $\Delta^9$ -*cis*-THC and ( $\pm$ )- $\Delta^9$ -*cis*-THC.

**CB1 and CB2 Binding Assay.** The assay was performed as previously described.<sup>22</sup> Briefly, 15  $\mu\text{g}$  of membrane preparation obtained from CHO cells stably transfected with *hCB1* or *hCB2* receptors was resuspended in 300  $\mu\text{L}$  of binding buffer [50 mM Tris-HCl, 2.5 mM EDTA, 5 mM MgCl<sub>2</sub>, and fatty-acid-free bovine serum albumin (BSA; 0.5 mg/mL) (pH 7.4)] in silanized glass tubes and co-incubated with the test compounds at different concentrations (1 pM to 100  $\mu\text{M}$ ) or vehicle and 0.5 nM [<sup>3</sup>H]CP55,940 (168 Ci/mmol) for 1.5 h at 30  $^{\circ}\text{C}$ . Nonspecific binding of the radioligand was determined in the presence of 10  $\mu\text{M}$  WIN55,512-2. After the incubation time, membrane suspensions were rapidly filtered through a 0.5% polyethylenimine-pres soaked 96-well microplate bonded with GF/B glass fiber filters (UniFilter-96 GF/B, PerkinElmer Life Sciences) under a vacuum and washed 12 times with 150  $\mu\text{L}$  of ice-cold washing buffer. Filters were added to 45  $\mu\text{L}$  of MicroScint-20 scintillation liquid, and radioactivity was measured with the 1450 MicroBeta Trilux top counter. Data were collected from at least three independent experiments performed in triplicate, and the nonspecific binding was subtracted. Results were expressed as [<sup>3</sup>H]CP55,940 bound as percentage of binding in vehicle-treated samples, and  $K_i$  (inhibition constant) values were calculated applying the Cheng–Prusoff equation.

**[<sup>35</sup>S]GTP $\gamma$ S Binding Assay.** The assay was performed as previously described.<sup>24</sup> Briefly, 5  $\mu\text{g}$  of clean membrane prepared in-house from CHO-*hCB2* and CHO-*hCB1* cells was diluted in silanized plastic tubes with 200  $\mu\text{L}$  of GTP $\gamma$ S binding buffer [50 mM Tris-HCl, 3 mM MgCl<sub>2</sub>, 0.2 mM EGTA, and 100 mM NaCl (pH 7.4) supplemented with 0.5% fatty-acid-free BSA] in the presence of 10  $\mu\text{M}$  GDP and 0.1 nM [<sup>35</sup>S]GTP $\gamma$ S (1250 Ci/mmol). The mixture was kept on ice until the binding reaction was started by adding the test compound, vehicle (negative control), or CP55,940 (positive control). Nonspecific binding was measured in the presence of 10  $\mu\text{M}$  GTP $\gamma$ S (Sigma). The tubes were incubated at 30  $^{\circ}\text{C}$  for 90 min under shaking, and then they were put on ice to stop the reaction. An aliquot (185  $\mu\text{L}$ ) of the reaction mixture was rapidly filtered through a 96-well microplate bonded with GF/B glass fiber filters (UniFilter-96 GF/B, PerkinElmer Life Sciences) previously presoaked with ice-cold washing buffer [50 mM Tris-HCl (pH 7.4) plus 0.1% fatty-acid-free BSA]. The filters were washed six times with 180  $\mu\text{L}$  of washing buffer under vacuum and dried under the air drier flow. The radioactivity

was measured with a 1450 Microbeta WallacTrilux Top counter after the addition of 45  $\mu\text{L}$  of scintillation cocktail. Specific binding was calculated by subtracting the residual radioactivity signal obtained in the presence of an excess of GTP $\gamma$ S, and the results were expressed as percentage of vehicle control.

**Enzymatic Assays.** FAAH, MAGL, and ABHDs activity assays were performed as previously described.<sup>22</sup> Briefly, FAAH and MAGL activity assays were performed using a U937 cell homogenate (100  $\mu\text{g}$ ), which were diluted in 200  $\mu\text{L}$  of 10 mM Tris-HCl and 1 mM EDTA, pH 8, containing 0.1% fatty-acid-free BSA. Compounds were added at the screening concentration of 10  $\mu\text{M}$  and incubated for 30 min at 37  $^{\circ}\text{C}$ . Then, 100 nM AEA containing 1 nM [ethanolamine-1-<sup>3</sup>H]AEA as a tracer for FAAH or 10  $\mu\text{M}$  2-oleoyl glycerol (2-OG) containing 1 nM [glycerol-1,2,3-<sup>3</sup>H]2-OG was added to the homogenates and incubated for 15 min at 37  $^{\circ}\text{C}$ . The reaction was stopped by the addition of 400  $\mu\text{L}$  of ice-cold CHCl<sub>3</sub>/MeOH (1:1), and samples were vortexed and rapidly centrifuged at 16000g for 10 min at 4  $^{\circ}\text{C}$ . The aqueous phases were collected, and the radioactivity was measured for tritium content by liquid scintillation spectroscopy. hABHD6 and hABHD12 activities were determined using cell homogenates from HEK-293 cells stably transfected with hABHD6 and hABHD12. Compounds were preincubated with 40  $\mu\text{g}$  of cell homogenate for 30 min at 37  $^{\circ}\text{C}$  in assay buffer (1 mM Tris and 10 mM EDTA plus 0.1% fatty-acid-free BSA, pH 7.6). DMSO was used as vehicle control with 10  $\mu\text{M}$  WWL70 or 20  $\mu\text{M}$  THL as positive controls for ABHD6 and ABHD12, respectively. Then, 10  $\mu\text{M}$  2-OG was added and incubated for 5 min at 37  $^{\circ}\text{C}$ . The reaction was stopped by the addition of 400  $\mu\text{L}$  of ice-cold CHCl<sub>3</sub>/MeOH (1:1). The samples were vortexed and centrifuged (16000g, 10 min, 4  $^{\circ}\text{C}$ ). Aliquots (200  $\mu\text{L}$ ) of the aqueous phase were assayed for tritium content by liquid scintillation spectroscopy. Blank values were recovered from tubes containing no enzyme. Basal 2-OG hydrolysis occurring in nontransfected HEK293 cells was subtracted. The experiments were performed at least two times in triplicate, and data are reported as mean values  $\pm$  SD.

**Animals.** In vivo experiments were performed in accordance with the Swiss Federal guidelines, which comply with the Institutional Animal Care and Use Committee (IACUC) guidelines. In particular, mice were handled according to Swiss Federal legislation, and protocols were approved by the respective government authorities (Veterinaramt Kanton Bern, experimental license BE-79/18). Male BALB/c mice (8 to 10 weeks old) were provided by Janvier Laboratories (St Berthevin, France). Mice were housed in groups of five per cage in a specific pathogen-free unit under controlled 12 h light/12 h dark cycle (ambient temperature, 21  $\pm$  2  $^{\circ}\text{C}$ ; humidity, 50–55%) with free access to standard rodent chow and water. The mice were acclimatized to the animal house for 1 week before the experiments.

**Tetrad Test.** Compounds were dissolved in pure DMSO and administered intraperitoneally at different doses using five to eight mice for each treatment group. ( $-$ )- $\Delta^9$ -*trans*-THC and ( $-$ )- $\Delta^9$ -*cis*-THC were administered 1 h before assessing locomotion, catalepsy, body temperature, and analgesia (collectively referred to as the tetrad test). The rectal temperature was measured before (basal) and 1 h after injection with a thermocouple probe (1 to 2 cm; Testo AG, Switzerland), and the change in rectal temperature was expressed as the difference between basal and postinjection temperatures. Catalepsy was measured using the bar test, where mice were retained in an imposed position with forelimbs resting on a bar 4 cm high; the end-point of catalepsy was considered when both front limbs were removed or remained over 120 s. Locomotion was determined using the rotarod test; animals were placed on the rotarod (Ugo Basile, Italy) at 6 rpm, and the latency to fall was measured with a cutoff time of 120 s. Catalepsy and locomotion were measured in three trials. The hot plate test was performed to evaluate analgesia using a 54–56  $^{\circ}\text{C}$  hot plate (Thermo Scientific) with a Plexiglas cylinder. The latency to the first nociceptive response (paw lick or foot shake) was measured.

**Statistical Analysis.** Data were collected from at least two independent experiments each performed in triplicate. Results are expressed as mean values and standard error deviation. The statistical

significance difference among groups was determined by non-parametric one-way ANOVA (Kruskal–Wallis test). Statistical differences between the treated and control groups were considered as significant if  $p < 0.05$ . GraphPad 8.0 software was used to fit the concentration-dependent curves and for the statistical analysis.

## ■ ASSOCIATED CONTENT

### SI Supporting Information

The Supporting Information is available free of charge at <https://pubs.acs.org/doi/10.1021/acs.jnatprod.1c00513>.

Mechanistic analysis of the reaction of olivetol and citral under acidic conditions;  $^1\text{H}$  NMR spectra of  $(-)\text{-}\Delta^9\text{-trans-THC}$ ,  $(-)\text{-}\Delta^9\text{-cis-THC}$ ,  $(+)\text{-}\Delta^9\text{-cis-THC}$ , and racemic  $\Delta^9\text{-cis-THC}$ ; ultraresolution separations of a  $\Delta^9\text{-trans-THC}$ -rich strain (Bedrocan) and a CBD-rich strain (Orange); main cannabinoids with their mass and highlighted isobaric compounds; ethanol extracts from Futura 75; extracted-ion chromatogram; eSFC separation of  $(\pm)\text{-}\Delta^9\text{-cis-THC}$  in fiber hemp strains; eSFC traces and extracted UV chromatograms of  $(\pm)\text{-}\Delta^9\text{-cis-THC}$  separation in fiber hemp strains (PDF)

## ■ AUTHOR INFORMATION

### Corresponding Authors

Jürg Gertsch – Institute of Biochemistry and Molecular Medicine, University of Bern, CH-3012 Bern, Switzerland; Phone: +41-31-6314111; Email: [juerg.gertsch@ibmm.unibe.ch](mailto:juerg.gertsch@ibmm.unibe.ch)

Erick M. Carreira – Laboratorium für Organische Chemie, ETH Zürich, 8093 Zürich, Switzerland; Phone: +41-44-6322830; Email: [erickm.carreira@org.chem.ethz.ch](mailto:erickm.carreira@org.chem.ethz.ch); Fax: +41-44-6321328

Giovanni Appendino – Dipartimento di Scienze del Farmaco, 28100 Novara, Italy; [orcid.org/0000-0002-4170-9919](https://orcid.org/0000-0002-4170-9919); Phone: +39-0321-375744; Email: [giovanni.appendino@uniupo.it](mailto:giovanni.appendino@uniupo.it); Fax: +39-0321-37564

### Authors

Michael A. Schafroth – Laboratorium für Organische Chemie, ETH Zürich, 8093 Zürich, Switzerland; [orcid.org/0000-0002-5864-6766](https://orcid.org/0000-0002-5864-6766)

Giulia Mazzocanti – Dipartimento di Chimica e Tecnologie del Farmaco, Sapienza Università di Roma, 00185 Rome, Italy

Ines Reynoso-Moreno – Institute of Biochemistry and Molecular Medicine, University of Bern, CH-3012 Bern, Switzerland

Reto Erni – Laboratorium für Organische Chemie, ETH Zürich, 8093 Zürich, Switzerland

Federica Pollastro – Dipartimento di Scienze del Farmaco, 28100 Novara, Italy; [orcid.org/0000-0002-0949-2799](https://orcid.org/0000-0002-0949-2799)

Diego Caprioglio – Dipartimento di Scienze del Farmaco, 28100 Novara, Italy

Bruno Botta – Dipartimento di Chimica e Tecnologie del Farmaco, Sapienza Università di Roma, 00185 Rome, Italy; [orcid.org/0000-0001-8707-4333](https://orcid.org/0000-0001-8707-4333)

Gianna Allegrone – Dipartimento di Scienze del Farmaco, 28100 Novara, Italy

Giulio Grassi – Canvasalus Research, 35043 Monselice, PD, Italy

Andrea Chicca – Institute of Biochemistry and Molecular Medicine, University of Bern, CH-3012 Bern, Switzerland; [orcid.org/0000-0001-9593-636X](https://orcid.org/0000-0001-9593-636X)

Francesco Gasparrini – Dipartimento di Chimica e Tecnologie del Farmaco, Sapienza Università di Roma, 00185 Rome, Italy; [orcid.org/0000-0003-0970-2917](https://orcid.org/0000-0003-0970-2917)

Complete contact information is available at: <https://pubs.acs.org/doi/10.1021/acs.jnatprod.1c00513>

### Author Contributions

<sup>1</sup>M.A.S., G.M., and I.R.-M. share first author status.

### Notes

The authors declare no competing financial interest.

## ■ ACKNOWLEDGMENTS

G.A. thanks MIUR for financial support to the groups in Novara (PRIN2017, Project 2017WN73PL, Bioactivity-directed exploration of the phytocannabinoid chemical space). We are grateful to Dr. Gianpaolo Grassi (Canvasalus) for the identification of all the plant material. The ETH group is grateful to the Swiss National Science Foundation for funding (2000020-172516)

## ■ REFERENCES

- (1) Adams, R.; Pease, D. C.; Cain, C. K.; Clark, J. H. *J. Am. Chem. Soc.* **1940**, *62*, 2402–2405.
- (2) Ghosh, R.; Todd, A. R.; Wright, D. C. *J. Chem. Soc.* **1941**, 137–140. The article by Todd appeared seven months after the one by Adams.
- (3) For a review on the early studies on cannabinoids, see: Appendino, G. *Rendiconti Lincei. Scienze Fisiche e Naturali* **2020**, *31*, 919–929.
- (4) Gaoni, Y.; Mechoulam, R. *J. Am. Chem. Soc.* **1964**, *86*, 1646–1647.
- (5) Santavý, F. *Acta Univ. Olomuc Fac. Med.* **1964**, *35*, 5–9.
- (6) Uliss, D. B.; Razdan, R. K.; Haldean, C.; Dalzell, G.; Handrick, R. *Tetrahedron Lett.* **1975**, *16*, 4369–4372.
- (7) Taylor, E. C.; Lenard, K.; Shvo, Y. *J. Am. Chem. Soc.* **1966**, *88*, 367–369.
- (8) Razdan, R. K.; Zitko, B. A. *Tetrahedron Lett.* **1969**, *10*, 4947–4950.
- (9) Uliss, D. B.; Handrick, G. R.; Dalzell, H. C.; Razdan, R. K. *Tetrahedron* **1978**, *34*, 1885–1888.
- (10) Smith, R. M.; Kempfert, K. D. *Phytochemistry* **1977**, *16*, 1088–1089.
- (11) WHO Expert Committee on Drug Dependence Fortieth Report. WHO Technical Report Series 1013. Geneva. Available at <https://apps.who.int/iris/bitstream/handle/10665/279948/9789241210225-engl.pdf>. Also DEA makes no distinction between stereoisomers of THC, only classifying positional isomers: [https://www.deadiversion.usdoj.gov/schedules/orangebook/c\\_cs\\_alpha.pdf](https://www.deadiversion.usdoj.gov/schedules/orangebook/c_cs_alpha.pdf).
- (12) Riboulet-Zemouli, K. *Drug Sci. Policy Law* **2020**, *6*, 1–37.
- (13) Edery, H.; Grunfeld, Y.; Ben-Zvi, Z.; Mechoulam, R. *Ann. N. Y. Acad. Sci.* **1971**, *191*, 40–53.
- (14) Martin, B. R.; Balstar, R. L.; Razdan, R. K.; Harris, L. S.; Dewey, W. L. *Life Sci.* **1981**, *29*, 565–574.
- (15) Yagen, B.; Mechoulam, R. *Tetrahedron Lett.* **1969**, *10*, 5353–5356.
- (16) (a) Schafroth, M. A.; Zuccarello, G.; Krautwald, S.; Sarlah, D.; Carreira, E. M. *Angew. Chem., Int. Ed.* **2014**, *53*, 13898–13901. (b) Krautwald, S.; Sarlah, D.; Schafroth, M. A.; Carreira, E. M. *Science* **2013**, *340*, 1065. (c) Krautwald, S.; Schafroth, M. A.; Sarlah, D.; Carreira, E. M. *J. Am. Chem. Soc.* **2014**, *136*, 3020. (d) Krautwald, S.; Carreira, E. M. *J. Am. Chem. Soc.* **2017**, *139*, 5627–5639.
- (17) Mazzocanti, G.; Ismail, O. H.; D'Acquarica, I.; Villani, C.; Manzo, C.; Wilcox, M.; Cavazzini, A.; Gasparrini, F. *Chem. Commun.* **2017**, *53*, 12262–12265.
- (18) (a) Badaloni, E.; Cabri, W.; Cioglia, A.; Deias, R.; Gasparrini, F.; Giorgi, F.; Vigevani, A.; Claudio Villani, C. *Anal. Chem.* **2007**, *79*,

6013–6019. (b) Badaloni, E.; Cabri, W.; Ciogli, A.; D'Acquarica, I.; Deias, R.; Gasparrini, F.; Giorgi, F.; Kotoni, D.; Villani, C. *J. Chromatogr A* **2010**, *1217*, 1024–1032.

(19) Schurig, V. *Molecules* **2016**, *21*, 1535.

(20) A most remarkable case is that of the polycyclic anticancer alkaloid cephalotaxine, in which the enantiomeric purity depends on the origin of its source plant, *Cephalotaxus harringtonii* (Forbes) K. Koch or *C. fortunei* Hook. (a) Robin, J.-P.; Blanchard, J.; Dhal, R.; Marie, J.-P.; Radosevic, N. US2004/0186095, 2004. (b) Huang, W.; Li, Y. X. *Sci. Sin. (Engl. Ed.)* **1980**, *23*, 835–840.

(21) Novak, A. J. E.; Trauner, D. *Trends Chem.* **2020**, *2*, 1052–1065.

(22) Chicca, A.; Nicolussi, S.; Bartholomäus, R.; Blunder, M.; Aparisi Rey, A.; Petrucci, V.; Reynoso-Moreno, I. D. C.; Viveros-Paredes, J. M.; Dalghi Gens, M.; Lutz, B.; Schiöth, H. B.; Soeberdt, M.; Abels, C.; Charles, R. P.; Altmann, K. H.; Gertsch, J. *Proc. Natl. Acad. Sci. U. S. A.* **2017**, *114*, 5006–5015.

(23) Pollastro, F.; Caprioglio, D.; Del Prete, D.; Rogati, F.; Minassi, A.; Tagliatalata-Scafati, O.; Muñoz, E.; Appendino, G. *Nat. Prod. Commun.* **2018**, *13*, 1189–1194.

(24) Chicca, A.; Schafroth, M.; Reynoso-Moreno, A.; Erni, R.; Petrucci, V.; Carreira, E. M.; Gertsch, J. *Sci. Adv.* **2018**, *4*, DOI: 10.1126/sciadv.aat2166.

(25) Lucas, C. J.; Galettis, P.; Schneider, J. *Br. J. Clin. Pharmacol.* **2018**, *84*, 2477–2482.

(26) (a) Gado, F.; Arena, C.; Fauci, C.; Reynoso-Moreno, I.; Bertini, S.; Digiaco, M.; Meini, S.; Poli, G.; Macchia, M.; Tuccinardi, T.; Gertsch, J.; Chicca, A.; Manera, C. *Bioorg. Chem.* **2020**, *17*, 103353. (b) Chicca, A.; Arena, C.; Bertini, S.; Gado, F.; Ciaglia, E.; Abate, M.; Digiaco, M.; Lapillo, M.; Poli, G.; Bifulco, M.; Macchia, M.; Tuccinardi, T.; Gertsch, J.; Manera, C. *Eur. J. Med. Chem.* **2018**, *154*, 155–171. (c) Chicca, A.; Caprioglio, D.; Minassi, A.; Petrucci, V.; Appendino, G.; Tagliatalata-Scafati, O.; Gertsch, J. *ACS Chem. Biol.* **2014**, *9*, 1499–507.

(27) (a) Waldman, M.; Hochhauser, E.; Fishbein, M.; Aravot, D.; Shainberg, A.; Sarne, Y. *Biochem. Pharmacol.* **2013**, *85*, 1626–1633. (b) Bilkei-Gorzo, O.; Albayram, A.; Draffehn, K.; Michel, A.; Piyanova, H.; Oppenheimer, M.; Dvir-Ginzberg, I.; Rác, T.; Ulas, S.; Imbeault, I.; Bab, J. L.; Schultze, A.; Zimmer, A. *Nat. Med.* **2017**, *23*, 782–787.

(28) Cook, C. E.; Seltzman, H. H.; Schindler, V. H.; Tallent, C. R.; Chin, K. M.; Pitt, C. G. *NIDA Res. Monogr.* **1982**, *42*, 19–32. Due to an easier synthesis, labeled ( $\pm$ )11-nor-9-carboxy-*cis*-THC acid glucuronide is currently used as an internal standard for (+)-*trans*-THC acid glucuronide in forensic tests of marijuana intoxication based on liquid chromatography–mass spectrometry (LC-MS). Grafinger, K. E.; Weinmann, W. J. *J. Anal. Toxicol.* **2021**, *45*, 291–296. This use is not recommended for immunoassay tests, but, if *cis*-THC is metabolized to its 11-nor-9-carboxy derivative like its *trans*-isomer, also the use in LC-MS becomes questionable.

(29) Citti, C.; Russo, F.; Sgrò, S.; Gallo, A.; Zanotto, A.; Forni, F.; Vandelli, M. A.; Laganà, A.; Montone, C. M.; Gigli, G.; Cannazza, G. *Anal. Bioanal. Chem.* **2020**, *412*, 4009–4022.

(30) Lewis, K.; Wagner, R.; Rodriguez-Cruz, S. E.; Weaver, M. J.; Dumke, J. C. *J. Forensic Sci.* **2021**, *66*, 285–294.

(31) Inspection of Table 1 shows that two varieties of fiber hemp (CRA\_5 Fibranova and Kompolti) would exceed the 0.3% legal threshold for “THC” if the *cis*-isomer is included in the account.